


## Article

# Factors Governing Site and Charge Density of Dissolved Natural Organic Matter

Rolf D. Vogt <sup>1,\*</sup> , Øyvind A. Garmo <sup>2</sup>, Kari Austnes <sup>1</sup>, Øyvind Kaste <sup>1</sup>, Ståle Haaland <sup>3</sup>, James E. Sample <sup>1</sup>, Jan-Erik Thrane <sup>1</sup>, Liv Bente Skancke <sup>1</sup>, Cathrine B. Gundersen <sup>1</sup> and Heleen A. de Wit <sup>1</sup>

<sup>1</sup> Norwegian Institute for Water Research, 0579 Oslo, Norway; kari.austnes@niva.no (K.A.); oeyvind.kaste@niva.no (Ø.K.); james.sample@niva.no (J.E.S.); jan-erik.thrane@niva.no (J.-E.T.); liv.skancke@niva.no (L.B.S.); cathrine.brecke.gundersen@niva.no (C.B.G.); heleen.de.wit@niva.no (H.A.d.W.)

<sup>2</sup> Sirkula IKS, 2301 Hamar, Norway; oyvind.garmo@sirkula.no

<sup>3</sup> Division of Environment and Natural Resources, Norwegian Institute of Bioeconomy Research, 1431 Ås, Norway; staale.haaland@nmbu.no

\* Correspondence: rolf.david.vogt@niva.no

**Abstract:** Rising organic charge in northern freshwaters is attributed to increasing levels of dissolved natural organic matter (DNOM) and changes in water chemistry. Organic charge concentration may be determined through charge balance calculations ( $\text{Org}^-$ ) or modelled ( $\text{OAN}^-$ ) using the Oliver and Hruška conceptual models, which are based on the density of weak acid functional sites (SD) present in DNOM. The charge density (CD) is governed by SD as well as protonation and complexation reactions on the functional groups. These models use SD as a key parameter to empirically fit the model to  $\text{Org}^-$ . Utilizing extensive water chemistry datasets, this study shows that spatial and temporal differences in SD and CD are influenced by variations in the humic-to-fulvic ratio of DNOM, organic aluminum (Al) complexation, and the mole fraction of CD to SD, which is governed by acidity. The median SD values obtained for 44 long-term monitored acid-sensitive lakes were 11.1 and 13.9  $\mu\text{Eq}/\text{mg C}$  for the Oliver and Hruška models, respectively. Over 34 years of monitoring, the CD increased by 70%, likely due to rising pH and declining Al complexation with DNOM. Present-day median SD values for the Oliver and Hruška models in 16 low-order streams are 13.8 and 15.8  $\mu\text{Eq}/\text{mg C}$ , respectively, and 10.8 and 12.5  $\mu\text{Eq}/\text{mg C}$ , respectively, in 10 high-order rivers.

**Keywords:** dissolved natural organic matter; organic charge; site density; charge density; Oliver model; Hruška model



**Citation:** Vogt, R.D.; Garmo, Ø.A.; Austnes, K.; Kaste, Ø.; Haaland, S.; Sample, J.E.; Thrane, J.-E.; Skancke, L.B.; Gundersen, C.B.; de Wit, H.A. Factors Governing Site and Charge Density of Dissolved Natural Organic Matter. *Water* **2024**, *16*, 1716. <https://doi.org/10.3390/w16121716>

Academic Editors: Anastasios Zouboulis and Yuanrong Zhu

Received: 6 April 2024  
Revised: 7 June 2024  
Accepted: 14 June 2024  
Published: 17 June 2024



**Copyright:** © 2024 by the authors. Licensee MDPI, Basel, Switzerland. This article is an open access article distributed under the terms and conditions of the Creative Commons Attribution (CC BY) license (<https://creativecommons.org/licenses/by/4.0/>).

## 1. Introduction

The concentrations of dissolved natural organic matter (DNOM) have increased in most northern freshwaters. This rise is attributed to several factors, including the reduced impact of acid rain [1], a warmer and wetter climate [2,3], and growing biomass [4,5], though not consistently [6]. Still, many acid-sensitive surface waters recovering from acid deposition are reverting from anthropogenic acidification to natural acidity [7], with the increased anionic charge from DNOM contributing considerably to the total anionic charge. The decline in acid rain, alongside other contributing factors, has amplified the relative and absolute significance of the organic charge stemming from the corresponding bases of weak acid functional groups present on DNOM.

Organic charge density (CD), which in this study refers to the concentration of calculated organic charge ( $\text{Org}^-$ ) normalized to the concentration of total organic carbon (TOC), is a conceptually important factor for understanding the solubility of DNOM and its function as a counter ion in the leaching of base cations and thus in the recovery from acid rain [7], as well as its role in the complexation and detoxification of heavy metals and aluminum (Al) [8]. For drinking water treatment plants that need to remove DNOM from their raw water, the CD of the DNOM plays a key role in governing treatability and

coagulant dose requirements [9]. Additionally, organic charge plays an important role in the quality control of major anion and cation data, as it significantly contributes to charge balance control, especially in dystrophic waters.

A modelled estimate of the organic charge concentration ( $\text{Org.}^-$ ) can be derived through conceptually formulated and empirically fitted models based on TOC, pH, and an estimate of the density of weak acid functional groups on the DNOM (SD). However, a challenge arises as this SD is hypothesized to differ spatially and vary over time, influenced by changes in the quality of DNOM and trends in the concentration of organically complexed aluminum. Consequently, there is a pressing need to elucidate the factors governing SD and CD and to gain a deeper understanding of their influence on these variables across space and time. Mindful of our extended use of abbreviations Table 1 provides a shortlist of commonly used shortenings.

**Table 1.** List of common abbreviations used throughout the text.

Abbreviation	Full Text	Meaning
DNOM	Dissolved natural organic matter	Humic and fulvic compounds
TOC	Total organic carbon	Concentration of organic carbon (C)
CD	Charge density	Anionic charge per mg C of DNOM
SD	Site density	Weak acid functional sites per mg C of DNOM
$\text{Org.}^-$	Organic charge	Organic charge based on ion balance including estimate of $\text{HCO}_3^-$
$\text{OAN}^-$	Organic anions	Modelled organic charge

Utilizing the vast expanse and diversity of monitoring data, this study establishes aggregated best estimates of the organic charge and interprets its main governing factors across space and time. Still, this study clearly reveals that more progress is needed to disclose the nature of SD and CD and their impacting factors.

## 2. Theory

### 2.1. Charge and Site Densities

Charge density (CD) is determined by normalizing  $\text{Org.}^-$  to the TOC concentration (i.e.,  $\frac{\text{Org.}^-}{\text{TOC}}$ ). The  $\text{Org.}^-$  is determined through ion balance calculations involving the molar equivalent charge of major cations and anions (i.e., calcium ( $\text{Ca}^{2+}$ ), magnesium ( $\text{Mg}^{2+}$ ), sodium ( $\text{Na}^+$ ), potassium ( $\text{K}^+$ ), ammonium ( $\text{NH}_4^+$ ), protons ( $\text{H}^+$ ), labile aluminum ( $\text{LAl}^{\text{n}+}$ ), sulphate ( $\text{SO}_4^{2-}$ ), nitrate ( $\text{NO}_3^-$ ), chloride ( $\text{Cl}^-$ ), and bicarbonate ( $\text{HCO}_3^-$ )). In cases where concentrations of  $\text{K}^+$ ,  $\text{NH}_4^+$ ,  $\text{LAl}^{\text{n}+}$ , and  $\text{HCO}_3^-$  are absent and negligible, they may be excluded. However, if the sample pH exceeds 5.5, a bicarbonate measure based on alkalinity readings must be factored into the calculation.

Brakke et al. [10], analyzing ion balance in water chemistry data from 94 dystrophic lakes across two regions of Norway (i.e., Gulsvik and Nord-Trøndelag), proposed the empirically fitted linear Equation (1) for estimating organic charge.

$$\text{Org.}^- = \text{CD} \cdot \text{TOC} - 0.96 \quad (1)$$

They reported the CD value as 4.06  $\mu\text{Eq}/\text{mg C}$ . This straightforward equation accounted for 55% of the variance in  $\text{Org.}^-$ . Similarly, Henriksen and Seip [11] reported a CD of 5.5  $\mu\text{Eq}/\text{mg C}$  based on extensive observations in lakes across Norway and Scotland in the late seventies, while Kortelainen [12] found a median CD of 7.5  $\mu\text{Eq}/\text{mg C}$  in a study of 955 Finnish lakes sampled in 1987.

Site density (SD) is used in conceptual organic acid models to characterize the relative abundance of weak organic acid functional groups (mainly carboxylic and phenolic acids) within the DNOM. SD can be determined through advanced measurements of the content of these acids in DNOM or, as undertaken in this study, it can be empirically calibrated

within the models by optimizing the model simulation of  $\text{OAN}^-$  relative to calculated  $\text{Org}^-$  across extensive datasets.

Based on the Gran titration of ion-exchanged samples, Hruška et al. [13] observed SD to be  $10.2 \mu\text{Eq}/\text{mg C}$  for Swedish sites and  $8.8 \mu\text{Eq}/\text{mg C}$  for the more acidified Czech sites. Oliver et al. [14] proposed an SD of  $10.5 \mu\text{Eq}/\text{mg C}$  ( $\pm 1.0$ ), derived from a weighted carboxylic content in humic and fulvic DNOM fractions in a limited number of XAD-8 isolated Canadian samples. Perdue and Richie [15], in a literature review of direct titrations of carboxylic and phenolic acid content in DNOM fractions, found lower mean densities of  $4.0$  and  $1.8 \mu\text{Eq}/\text{mg C}$  for carboxylic and phenolic acid groups in humic acids, respectively, compared to  $5.1$  and  $1.7 \mu\text{Eq}/\text{mg C}$  for fulvic acids. Given DNOM's blend of humic and fulvic acids, the concentration of carboxylic and phenolic acids in the DNOM was measured at  $5.2$  and  $1.9 \mu\text{Eq}/\text{mg C}$ , respectively.

Within the fulvic DNOM fraction, Perdue and Richie [15] suggested a higher SD of weak acid functional groups, such as carboxylic and phenolic acids, compared to the humic fraction. Additionally, they documented a greater level of aromaticity in the humic fraction compared to the fulvic fraction. Aromatic compounds, rich in conjugated double bonds, absorb UV light and wavelengths ( $\lambda$ ) into the visible (VIS) light spectrum. Wavelengths of  $254$  and  $410$  nm are thus widely used as proxies for DNOM, and their specific absorbencies ( $s\text{UVa}$  and  $s\text{VISa}$ ) are positively correlated to DNOM aromaticity and, consequently, to the ratio of humic to fulvic fractions in the DNOM ([16] and references therein). Based on this conceptual framework, one could hypothesize that the SD of DNOM decreases with increasing  $s\text{UVa}$  and  $s\text{VISa}$ .

In summary, the SD and CD of DNOM exhibit significant spatial and temporal variability and their estimates depend on the methodology employed for their determination.

## 2.2. Organic Charge Models

Assuming a triprotic model, Lydersen et al. [8] proposed Equation (2) for  $\text{OAN}^-$  by simply assuming one-third of the SD as strong acid anions.

$$\text{OAN}^- = \frac{\text{SD} \cdot \text{TOC}}{3} \quad (2)$$

This equation has been utilized in critical load assessments [17] to improve the ecological relevance of the acid-neutralizing capacity (ANC) using organic acid-adjusted ANC ( $\text{ANC}_{\text{OAA}} = \text{ANC} - \text{OAN}^-$ ). Still, the actual mole fraction ( $\alpha$ ) of charged functional groups hinges on the protonation level of the organic acids and their complexation with aluminum and partly iron (Fe). Consequently, the CD is governed by the SD and influenced by factors such as pH and metal complexation. CD is thus lower than or equal to SD due to the presence of protonated sites or complexes with Al and Fe.

Prominent models accounting for the effect of pH variations on CD include the Oliver model [14] and the Hruška model [13]. These conceptual frameworks simulate the concentration of organic charge ( $\text{OAN}^-$ ) based on TOC, pH, and a selected SD. The Oliver model is given in Equation (3).

$$\text{OAN}^- = \text{TOC} \cdot \text{SD} \cdot \frac{10^{-(0.96+0.9 \cdot \text{pH}-0.039 \cdot \text{pH}^2)}}{10^{-(0.96+0.9 \cdot \text{pH}-0.039 \cdot \text{pH}^2)} + 10^{-\text{pH}}} \quad (3)$$

Here, the fraction expression denotes the mole fraction ( $\alpha$ ) for the overall protolysation ratio (i.e.,  $\text{CD}/\text{SD}$ ). Spatial disparities and temporal changes in SD may be accommodated by adjusting this parameter within the models.

The Hruška model is based on the definitions of mole fractions ( $\alpha$ ) of the protonated acids considering the organic acids in the DNOM as triprotic (Equations (4)–(7)).

$$\alpha_0 = \frac{(10^{-\text{pH}})^3}{(10^{-\text{pH}})^3 + 10^{-\text{pK}_{a1}} \cdot 10^{-\text{pK}_{a2}} \cdot 10^{-\text{pH}} + 10^{-\text{pK}_{a1}} \cdot 10^{-\text{pK}_{a2}} \cdot 10^{-\text{pK}_{a3}}} \quad (4)$$

$$\alpha_1 = \frac{10^{-\text{pK}_{a1}} \cdot \alpha_0}{10^{-\text{pH}}} \quad (5)$$

$$\alpha_2 = \frac{10^{-\text{pK}_{a1}} \cdot 10^{-\text{pK}_{a2}} \cdot \alpha_0}{(10^{-\text{pH}})^2} \quad (6)$$

$$\alpha_3 = \frac{10^{-\text{pK}_{a1}} \cdot 10^{-\text{pK}_{a2}} \cdot 10^{-\text{pK}_{a3}} \cdot \alpha_0}{(10^{-\text{pH}})^3} \quad (7)$$

Here,  $\alpha_0$ ,  $\alpha_1$ ,  $\alpha_2$ , and  $\alpha_3$  denote the relative fractions of  $\text{H}_3\text{A}$ ,  $\text{H}_2\text{A}^-$ ,  $\text{HA}^{2-}$ , and  $\text{A}^{3-}$ , respectively. For Swedish sites, the following constants were calibrated:  $\text{pK}_{a1} = 3.04$ ,  $\text{pK}_{a2} = 4.51$ , and  $\text{pK}_{a3} = 6.46$ . Meanwhile, the constants for Czech sites were the following:  $\text{pK}_{a1} = 2.5$ ,  $\text{pK}_{a2} = 4.42$ , and  $\text{pK}_{a3} = 6.7$ . The median difference in fitted SD values using the two different  $\text{pK}_a$  sets is negligible, e.g., only a median of 0.88  $\mu\text{Eq}/\text{mg C}$  (2.7%) in the ICP Waters data set (i.e., introduced below). For consistency, we have therefore in this study only used the  $\text{pK}_a$  values for the Swedish sites.

The  $\text{OAN}^-$  is then calculated as given in Equation (8).

$$\text{OAN}^- = \text{TOC} \cdot \left( \frac{\alpha_1 \cdot \text{SD}}{3} + \frac{2 \cdot \alpha_2 \cdot \text{SD}}{3} + \frac{3 \cdot \alpha_3 \cdot \text{SD}}{3} \right) \quad (8)$$

Other useful models for estimating the charge of organic matter, as documented in the scientific literature, include those proposed by Driscoll et al. [18], the ALCHEMY di- and triprotic model by Schecher and Driscoll [19], the DOM fraction model by Kortelainen [20], and the chemical equilibrium models WHAM and NICA-Donnan by Tipping [21,22] and Kinniburgh et al. [23], respectively.

To our knowledge, there exists no previous studies that seek to establish an overview of suitable SDs to be applied in the Oliver and Hruška models for generating estimates of organic charge concentration. This is sought for, as the relative contribution of organic charge is increasing with declined acid rain and increasing DOM with climate change and increased biomass.

### 3. Materials and Methods

#### 3.1. Data Mining

The data utilized in this study are derived from several extensive monitoring programs, encompassing the ICP Waters data [24] including data for the Norwegian ØkoForsk Trend and research monitoring stations, Reference Streams [25], and the Norwegian River monitoring program [26], as well as the 1000 Lakes study [3], commissioned by the Norwegian Environment Agency. The ICP Waters monitoring dataset consists of 73,656 samples collected between 1990 and 2020 from 430 sites across Europe and Northeastern America. The ØkoForsk Trend program has been conducting annual water chemistry monitoring at 78 acid-sensitive Trend Lakes since 1986 and weekly water chemistry monitoring, including alkalinity, at six research sites since 2001. Data from the Reference Streams monitoring program include observations from 80 streams with different land uses sampled monthly and bi-annually since 2017. The Norwegian River monitoring program, including alkalinity since 2021, monitors 22 rivers along the Norwegian coast monthly for physical and chemical parameters. The 1000 Lakes study, conducted in the fall of 2019, sampled 2.5% of all lakes in Norway with a surface area larger than 0.04  $\text{km}^2$ . The sampled lakes were distributed in a ratio of 3:2:1 among lakes from southern, middle, and northern Norway, respectively. All data for the Norwegian sites are available from the Norwegian Environment Agency [27].

#### 3.2. Calculation of Organic Charge

The concentration of  $\text{Org}^-$  is calculated based on charge balance principles. Below a pH of 5.5, it is assumed that there is a negligible carbonate alkalinity. However, above this threshold,  $\text{HCO}_3^-$  significantly contributes to alkalinity (i.e.,  $\alpha_1 > 0.15$ ). Total alkalinity data are then utilized to estimate the concentration of weak acids, primarily  $\text{HCO}_3^-$  and

Org.<sup>-</sup>. Distinguishing between bicarbonate alkalinity and organic alkalinity in alkalinity measurements is challenging. In samples with pH above 5.5, the HCO<sub>3</sub><sup>-</sup> concentration is calculated using Equation (9), derived from [28].

$$[\text{HCO}_3^-] = \text{Alkalinity} - \left( \text{OAN}^-_{\text{Sample pH}} - \text{OAN}^-_{\text{pH4.5}} \right) - 31.62 + 0.2 \cdot \sqrt{\text{Alkalinity} - 31.6} \quad (9)$$

In this context, “Alkalinity” refers to the measured total alkalinity [29], “OAN<sup>-</sup><sub>Sample pH</sub>” represents the modelled organic charge using either the Oliver or Hruška model at the sample pH, and “OAN<sup>-</sup><sub>pH4.5</sub>” indicates the respective modelled organic charge at pH 4.5. The value 31.62 signifies the concentration of H<sup>+</sup> ions at the titration endpoint (pH 4.5). All concentrations are expressed in μEq/L. The contribution of organic alkalinity to total alkalinity measurements is usually minor, encompassing solely the protonation of organic charge from the sample pH to pH 4.5 [28]. Nevertheless, determining the OAN<sup>-</sup> at sample pH and pH 4.5 to calculate the difference and thus its contribution to measured alkalinity entails a somewhat circular argument in our deductions. Additionally, it is necessary to subtract the contribution to alkalinity caused by the addition of acid to adjust the sample pH from the equivalence pH to pH 4.5.

When aiming to determine an optimal SD that establishes a 1:1 relationship between modelled OAN<sup>-</sup> and calculated Org.<sup>-</sup>, conceived as true value, the circular argument mentioned above poses a significant challenge. This is because increasing the SD concurrently elevates both the OAN<sup>-</sup> and Org.<sup>-</sup> in scenarios with carbonate alkalinity. To circumvent this issue in calculations, using Equation (9), we fixed the SD values in the Oliver (Equation (3)) and Hruška models (Equation (8)) at their literature values 10.5 and 10.2 μEq/mg C, respectively. This approach ensures that the circular argument is mitigated when calculating the difference between OAN<sup>-</sup><sub>Sample pH</sub> and OAN<sup>-</sup><sub>pH 4.5</sub> in Equation (9), thereby accounting for the contribution of organic charge to measured alkalinity.

By estimating the concentration of bicarbonate using Equation (9), the Org.<sup>-</sup> concentration can be deduced based on the anion deficit in the charge balance. If there is no anion deficit, the concentration of Org.<sup>-</sup> is assumed to be negligible and the value for Org.<sup>-</sup> is set to zero and omitted in the regressions.

The sUVa and sVISA are the absorbency at λ254 and λ410 nm, respectively, normalized to the TOC concentration. In the Reference Stream dataset, the sVISA is based on the Color number (i.e., Platinum number) linearly converted to absorbency at λ410 nm. The quantity of aluminum (Al) complexed to the DNOM is indirectly assessed by the concentration ratio of reactive Al (RAI) or directly by the ratio of non-labile Al (ILAl) to the TOC.

All calculations were conducted using Microsoft Excel, while statistical analysis was performed using MINITAB (2021).

### 3.3. Determining Site Density through Model Optimization

The models are calibrated by fitting the SD to achieve an optimal accuracy (i.e., OAN<sup>-</sup> = Org.<sup>-</sup>) by finding the SD that gives a 1:1 linear correlation anchored through the origin (i.e., slope of 1) between OAN<sup>-</sup> and Org.<sup>-</sup>. Forcing the linear slope through the origin minimizes the effect of poor model accuracy at low Org.<sup>-</sup>.

### 3.4. Limitations in the Conceptual Approach

The calculation of Org.<sup>-</sup> entails considerable uncertainties, given that it represents a small difference between the substantial sums of major cations and anions, compounded by the inherent propagation of analytical errors in their constituents and in alkalinity measurements. Furthermore, uncertainties also arise from assumptions employed to calculate HCO<sub>3</sub><sup>-</sup> from alkalinity (Equation (9)) and in the approach for assessing the protonation of organic charge from sample pH to pH 4.5. Consequently, calculated HCO<sub>3</sub><sup>-</sup> concentrations can be somewhat overestimated in samples with low DNOM concentrations and may hence lead to a calculated apparent cation deficiency. In this study, the concentration of Org.<sup>-</sup> is then omitted from the regression assessment, as their concentrations are assumed

insignificant and irrelevant. In assessments of median  $\text{Org.}^-$  and CD values, the  $\text{Org.}^-$  concentrations were set to zero in samples with a positive charge balance.

In addition to uncertainties in  $\text{Org.}^-$  calculation, there are inherent limitations to the modelled  $\text{OAN}^-$ , as the model solely relies on a pH-governed mole fraction ( $\alpha$ ) of the CD to SD ratio, without accounting for the effects of Al and Fe complexation. Furthermore, analytical uncertainties in determining TOC and pH add to the overall uncertainty. Generally, the models are found to generate too high an  $\text{OAN}^-$  at calculated  $\text{Org.}^-$  values less than  $20 \mu\text{Eq/L}$ .

## 4. Results and Discussion

### 4.1. Comparison of $\text{OAN}^-$ Based on Oliver and Hruška Models

The ICP Waters dataset [24] serves as an invaluable resource for evaluating model performance across a broad spectrum of parameter values as well as temporal and spatial dimensions. The model-derived organic charge concentrations ( $\text{OAN}^-$ ) based on the Oliver (Equation (3)) and Hruška models (Equation (8)) are strongly correlated ( $R^2 = 0.9948$ , Figure 1). When employing SDs of  $10.5$  and  $10.2 \mu\text{Eq/mg C}$ , as proposed by Oliver et al. [14] and Hruška et al. [13], respectively, the regression slope is  $0.80$ . This indicates that although the precision among these models is excellent, the accuracy is poor, with the  $\text{OAN}^-$  simulated by the Oliver model being approximately 20% higher than that of the Hruška model. Decreasing the Oliver model's SD to  $8.43 \mu\text{Eq/mg C}$  yields a 1:1 relationship with the Hruška model set at  $\text{SD} = 10.2 \mu\text{Eq/mg C}$  (Figure 1). From this, we infer that these models demonstrate strong compatibility, despite notable disparities in the SD values utilized to calibrate them. In this study, the estimated SDs for both models are therefore assessed.

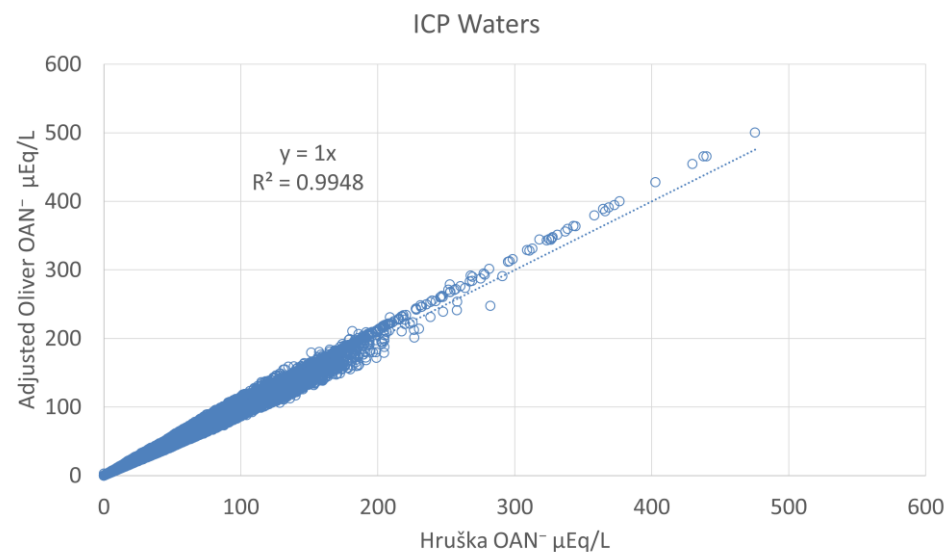


**Figure 1.** Correlation between the  $\text{OAN}^-$  values estimated using the Oliver model (Equation (3)) with an adjusted SD of  $8.43 \mu\text{Eq/mg C}$  vs. the Hruška model (Equation (8)) with an  $\text{SD} = 10.2 \mu\text{Eq/mg C}$  on the ICP Waters data.

### 4.2. Comparison of Modelled $\text{OAN}^-$ with Calculated $\text{Org.}^-$

For the 1000 Lakes samples [3], with total organic carbon (TOC) concentrations above  $1 \text{ mg C/L}$ , the optimized SDs for the Oliver and Hruška models, achieving a 1:1 relationship between  $\text{OAN}^-$  and  $\text{Org.}^-$  (Figure 2), were  $19.0$  and  $29.0 \mu\text{Eq/mg C}$ , respectively. However, these overall SD values, assessed across sites with varying SDs, appear notably high compared to the calculated average charge density (CD) values of  $11.2$  and  $11.9 \mu\text{Eq/mg C}$ . This discrepancy arises from the inclusion of many sites where the models fail to accurately simulate the data, indicated by a coefficient of determination ( $R^2$ ) below  $0.75$ . Moreover, 63% of the samples had no or insignificant organic charge; thus,  $\text{Org.}^-$  values were set

to zero. Despite these discrepancies, it is noteworthy that 71% of the  $\text{Org.}^-$  in these 1000 Lakes remains unprotonated at pH 4.5. Consequently, this discrepancy does not significantly impede the comparison between the modelled organic acid anion ( $\text{OAN}^-$ ) and calculated  $\text{Org.}^-$  based on charge balance, which includes  $\text{HCO}_3^-$  calculated from alkalinity using Equation (9).

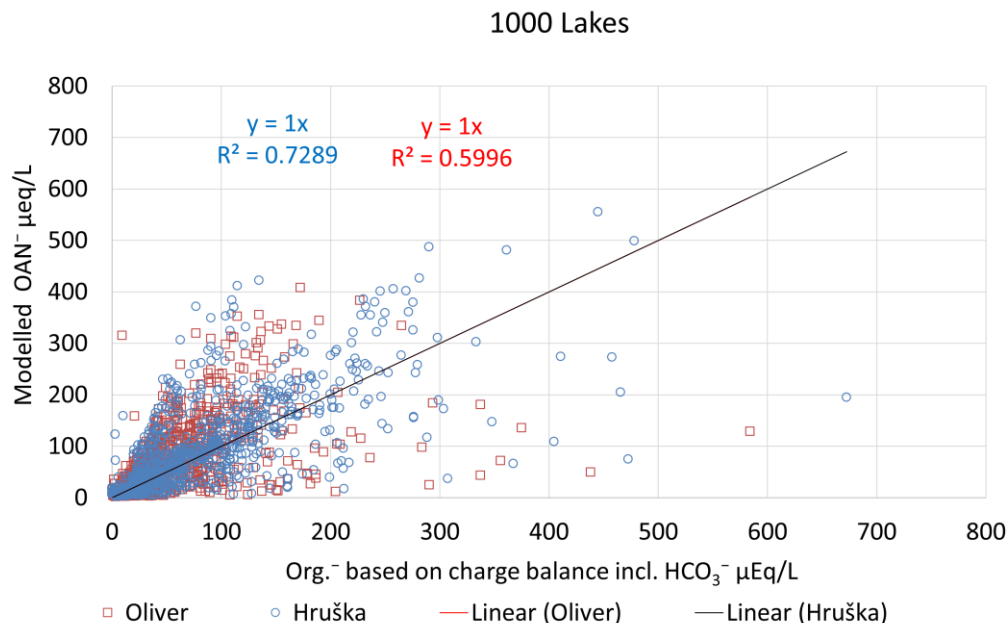


**Figure 2.** Modelled  $\text{OAN}^-$  by Oliver and Hruška models vs. “true”  $\text{Org.}^-$  calculated on the 1000 Lakes samples, with TOC concentrations higher than 1 mg C/L, with an optimized SD rendering a 1:1 relationship (line) anchored through the origin. The  $\text{Org.}^-$  is based on charge balance including bicarbonate (from Equation (9)).

Although the Oliver and Hruška models, when optimized for the 1000 Lakes data, yield reasonably acceptable simulations of  $\text{OAN}^-$  concentrations, explaining 65% and 72% of the variation in  $\text{Org.}^-$ , respectively, it is evident from Figure 2 that there exist subsets of sites with markedly different SDs, leading to varying  $\text{OAN}^-$  to  $\text{Org.}^-$  ratios. Clusters exhibiting high ratios likely correspond to sites where the models fail to perform effectively. To establish a more accurate estimate for SDs to be used in the Oliver and Hruška models, it becomes vital to optimize the SD based on temporal variations in TOC concentrations and pH relative to  $\text{Org.}^-$  at individual sites.

#### 4.3. Governing Factors for Site and Charge Densities

The site-optimized SD in the models using data from 78 Trend Lakes and 80 Reference Streams reveals an exponential increase in SD with declining TOC (Figure 3). This trend is partially mechanistically sound, as the proportion of humic to fulvic fraction generally decreases with decreasing TOC, leading to an increase in the SD of the DNOM. However, sites with a coefficient of determination ( $R^2$ ) dropping below 0.75 for the correlation between modelled  $\text{OAN}^-$  and calculated  $\text{Org.}^-$  exhibit large scatter in the SD with some unrealistically high SDs (e.g., >20  $\mu\text{Eq}/\text{mg C}$ ), particularly evident at sites with low TOC concentrations (Figure 3). Furthermore, the relationship between hydrogen ion concentration ( $\text{H}^+$ ) and SD demonstrates significant variability in SD at pH levels above 5.5 (i.e.,  $\text{H}^+ < 3.2 \mu\text{Eq}/\text{L}$ ). At these pH levels, the levels of  $\text{HCO}_3^-$  constitute a substantial contribution to the charge balance, consequently affecting  $\text{Org.}^-$  levels. Thus, the steep increase in SD at low TOC concentrations likely reflects limitations in the adopted conceptual approach. Total reactive aluminum concentrations (RAI) follow similar trends with SD as  $\text{H}^+$  (Figure 3), partly due to the covariance between  $\text{H}^+$  and RAI resulting from the pH dependence on aluminum solubility, as well as reflecting a dependence of organic Al

complexation. These anomalies lead to the models generally overestimating the  $\text{OAN}^-$  at low concentrations of  $\text{Org.}^-$  ( $<20 \mu\text{Eq/L}$ ).

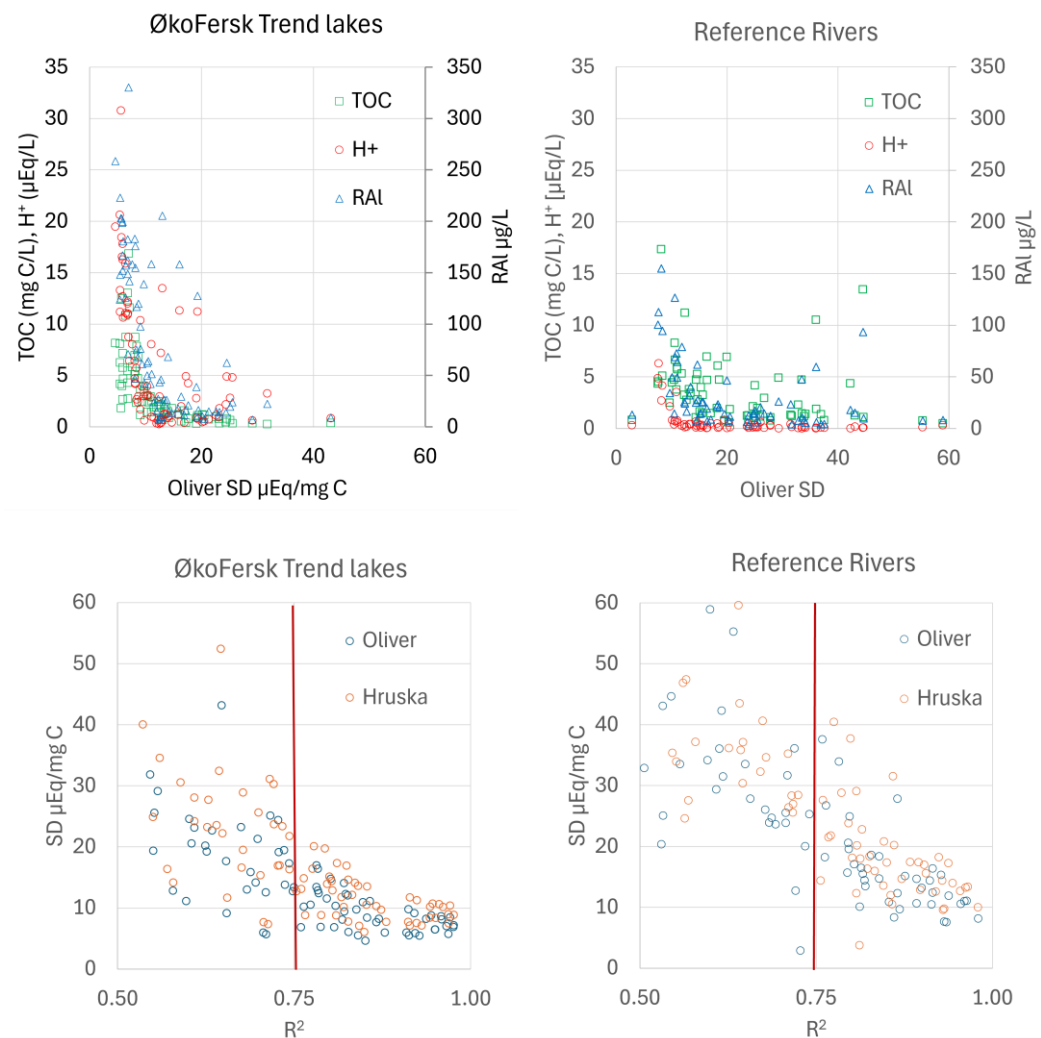


**Figure 3.** Relationship between the site average levels of TOC, H<sup>+</sup>, and RAI vs. the optimized SD for the Oliver model (**top**) and the dependence of SD on the coefficient of determination (R<sup>2</sup>), based on optimized model simulations of the Oliver and Hruška models (**bottom**) in 78 Trend Lakes (**left**) and 80 Reference Streams (**right**).

In summary, sites with low TOC concentrations inherently exhibit low  $\text{OAN}^-$ . Coupled with relatively high uncertainty in calculating low  $\text{Org.}^-$  concentrations, this results in the highly uncertain optimization of site density (SD). Consequently, from the subsequent optimization of SDs, we have excluded sites in the linear correlations where the median TOC concentration is below 1 mg C/L and/or where R<sup>2</sup> fails to exceed 0.75.

#### 4.4. Spatiotemporal Variations in Functional Site Density

To establish site-specific SDs, the values were optimized within the Oliver and Hruška models by fitting  $\text{OAN}^-$  to  $\text{Org.}^-$  using long-term variations in data for explanatory variables, including alkalinity, sourced from the 78 Trend Lakes and the 6 Research Monitoring Sites in the ØkoFersk Trend monitoring program (data from [24]), as well as the 80 Reference Streams [25] and 22 major rivers draining into coastal waters [26].

After excluding sites with median TOC concentrations less than 1 mg C/L and coefficient of determination (R<sup>2</sup>) values below 0.75 in the ØkoFersk Trend Lakes and Reference Stream datasets, 44 and 35 sites were retained, respectively. In Trend Lake sites where



the models failed to achieve an explanatory value greater than 75%, the acid-neutralizing capacity (ANC) was low or negative, indicating low or negligible  $\text{Org.}^-$  content. Conversely, Reference Stream sites where the models failed were characterized by significantly higher alkalinity values and base cation concentrations, indicating water with high levels of bicarbonate and hard water. The median SD achieved during model optimization was  $11.1 \mu\text{Eq}/\text{mg C}$  for the Oliver model and  $13.9 \mu\text{Eq}/\text{mg C}$  for the Hruška model in the acid-sensitive Trend Lakes and  $14.4 \mu\text{Eq}/\text{mg C}$  for the Oliver model and  $16.3 \mu\text{Eq}/\text{mg C}$  for the Hruška model in Reference Streams. Over time, these SD values have shown an increase during the monitoring period for the Trend Lakes, as assessed below. Hence, these SD values represent median spatiotemporal values.

Spatial variations in SD in the cleaned long-term dataset from Trend Lake and Reference Streams sites are primarily governed by differences in site average TOC,  $\text{H}^+$ , and reactive aluminum (RAI) concentrations (Figure 4). Data generated by the Hruška model yield similar results (not displayed). The observed increase in SD with decreasing TOC and  $\text{H}^+$  concentration is likely attributed to the relatively higher fraction of fulvic compared to humic moieties in the DNOM at sites with lower TOC concentrations, as elaborated below. The increase in apparent SD with decreasing RAI may partly be explained by reduced organic complexation with Al.

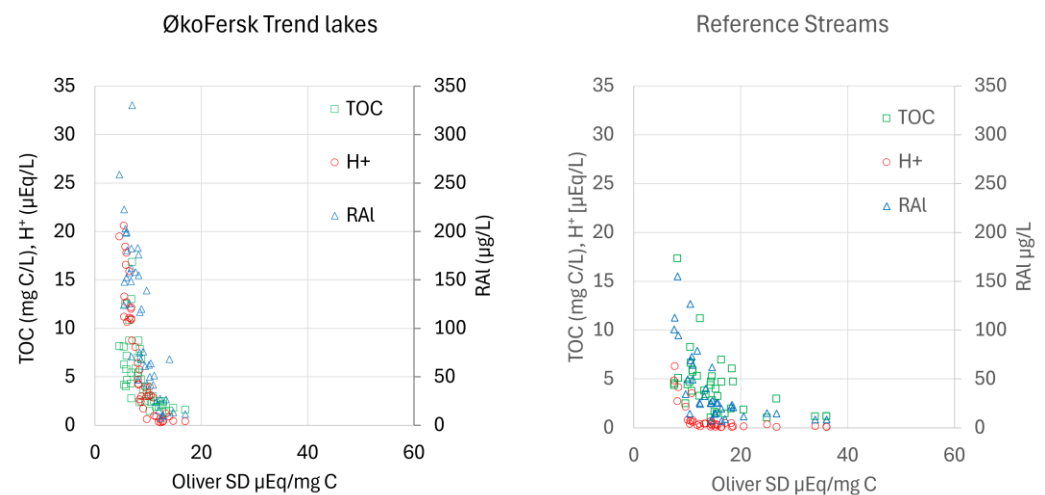


**Figure 4.** Relationship between the site average levels of TOC,  $\text{H}^+$ , and RAI vs. the optimized SD using the Oliver model in 44 ØkoFersk Trend Lakes since 1986 and 35 Reference Streams since 2007 at sites with average TOC  $> 1 \text{ mg C}/\text{L}$  and an  $R^2 > 0.75$  of the correlation between  $\text{OAN}^-$  and  $\text{Org.}^-$ .

The spatial disparity in Oliver SD is predominantly explained by variations in site-specific factors such as average  $\text{H}^+$ , RAI, and TOC concentrations, which reflect differences in the quality of DNOM. A multiple linear regression model incorporating  $\text{H}^+$  and TOC accounts for 74% and 41% of the SD variance across the 44 Trend Lakes (Equation (10)) and 35 Reference Streams (Equation (11)), respectively.

$$\text{SD} = 14.63 - 0.3699 \cdot \text{H}^+ - 0.2153 \cdot \text{TOC} \quad (10)$$

$$\text{SD} = 19.20 - 1.723 \cdot \text{H}^+ - 0.6590 \cdot \text{TOC} \quad (11)$$

Here, the  $\text{H}^+$  concentration is denoted in  $\mu\text{Eq}/\text{L}$ , while TOC is measured in  $\text{mg C}/\text{L}$ . The  $p$ -value associated with TOC in Equation (10) exceeds 0.05, indicating its poor significance. This equation fails to effectively model SD beyond the threshold of  $12 \mu\text{Eq}/\text{mg C}$ , a limitation evident from Figures 3 and 4. By substituting TOC with the less commonly measured RAI in the multiple linear regression analysis for the Trend Lakes, a stronger equation (Equation (12)) emerges, explaining a slightly higher proportion (78%) of the variance. Notably, all parameters exhibit significance. However, when applying this substi-

tution to the data from Reference Streams, which encompass less acid-sensitive sites with a median pH of 6.4, the model's performance does not improve.

$$SD = 14.805 - 0.2935 \cdot H^+ - 0.01628 \cdot RAI \quad (12)$$

The spatial variability in SD, as derived from data collected at the 6 Research Monitoring Sites, which contain alkalinity data since 2001, is detailed in Table 2. Among these sites, the SD was primarily governed by pH and TOC, rather than RAI. Notably, there exists a robust positive correlation between SD and the average pH of the sites ( $R^2 = 0.8295$ ), alongside a negative correlation with average TOC concentrations ( $R^2 = 0.5964$ ). Conversely, sulphate ( $SO_4^{2-}$ ) concentrations demonstrate negligible explanatory power. This can be attributed to the limited number of research monitoring sites, which encompass a broad range of acid sensitivities. For instance, the Dalelva site, despite exhibiting high sulphate levels due to acid oxide pollution from nearby metal smelters in Nikel, Russia, is well-buffered, displaying high pH values and low RAI concentrations. On the other hand, Kårvatn, which has the highest SD (19.1  $\mu\text{Eq}/\text{mg C}$ ), is a less acid-sensitive site and is exposed to the lowest levels of acid rain, reflected by high pH and low RAI, as well as low TOC (Table 2). This aligns with the understanding that acid rain, along with DNOM levels, are important drivers for SD.

**Table 2.** Optimized SD (Oliver model) for the modelled  $OAN^-$ , i.e., generating a correlation slope of 1.000 against calculated  $Org.^-$  based on IB including  $HCO_3^-$  estimated using Equation (9), on weekly data since 2001 from the 6 intensively monitored research stations in ØkoForsk Trend, along with main median explanatory parameters and the resulting sample median CD (i.e.,  $Org.^- / TOC$ ). pH is based on the median  $H^+$  concentration.

Site	No. samples #	Measured				Calculated		Oliver Modelled		$R^2$
		$SO_4^{2-}$ $\frac{Eq}{L}$	pH	TOC $\frac{mg\ C}{L}$	RAI $\frac{\xi}{L}$	$Org.^-$ $\frac{Eq}{L}$	CD $\frac{Eq}{mg\ C}$	$OAN^-$ $\frac{Eq}{L}$	SD $\frac{Eq}{mg\ C}$	
Birkenes	1083	48.5	4.88	5.7	270	14.8	2.49	22	5.31	0.7781
Øygardsbekken	826	34.8	5.49	1.5	58	7.37	4.23	15	11.7	0.5703
Langtjern	1086	16.3	5.05	11	155	59.8	5.25	61	6.88	0.9892
Storgama	1047	14.3	5.00	6.2	103	27.1	4.30	28	5.97	0.9585
Kårvatn	806	12.5	6.39	0.87	14	13.7	14.8	18	19.1	0.7426
Dalelva	1081	77.5	6.37	3.4	34	37.8	10.9	43	12.6	0.8625

Optimizing the SD for the modelled  $OAN^-$  to  $Org.^-$  data obtained from each of the Research Monitoring Stations yields a range of values spanning from 5 to 19  $\mu\text{Eq}/\text{mg C}$  (Table 2). Inherently, the Oliver model tends to exhibit limited explanatory power at Research Monitoring Sites characterized by low  $Org.^-$  levels, such as Øygardsbekken and Kårvatn (Table 2). Conversely, stronger explanatory values ( $R^2$ ) are observed at dystrophic sites boasting high TOC concentrations, such as Langtjern and Storgama. However, at Birkenes, despite relatively high TOC levels, the correlation remains relatively poor due to the low CD of the organic matter (2.5  $\mu\text{Eq}/\text{mg C}$ ).

#### 4.5. Spatial Differences in Contemporary Site Density

The SDs based on recent seasonal fluctuations in monthly samples collected in 2022 from 37 Reference Streams [25] are devoid of long-term temporal trends in the SD. A total of 21 streams were excluded from this analysis due to TOC concentrations less than 1 mg C/L and/or  $R^2$  poorer than 0.75. Within this dataset, the median SDs for the remaining 16 Reference Streams, when employing the Oliver and Hruška models, stand at 13.8  $\mu\text{Eq}/\text{mg C}$  (STD: 4.5  $\mu\text{Eq}/\text{mg C}$ ) and 15.8  $\mu\text{Eq}/\text{mg C}$  (STD: 4.8  $\mu\text{Eq}/\text{mg C}$ ), respectively. The relatively high SD observed in this 2022 dataset, compared to the time-averaged SD from long-term monitoring data collected from the Trend Lakes, aligns with a trend of increasing CD over time as assessed below. Spatial differences in SD are significantly correlated with the site average concentrations of TOC and RAI, explaining 21% and 17% of the variation in SD,

respectively (Figure 5). The explanatory power of  $H^+$  for spatial variation in SD is limited due to the higher pH (ranging in median values from 5.2 to 7.3) observed among these Reference Streams, which exhibit varying land use, compared to the more consistently acid-sensitive Trend Lakes characterized by a median pH ranging from 4.7 to 6.6.

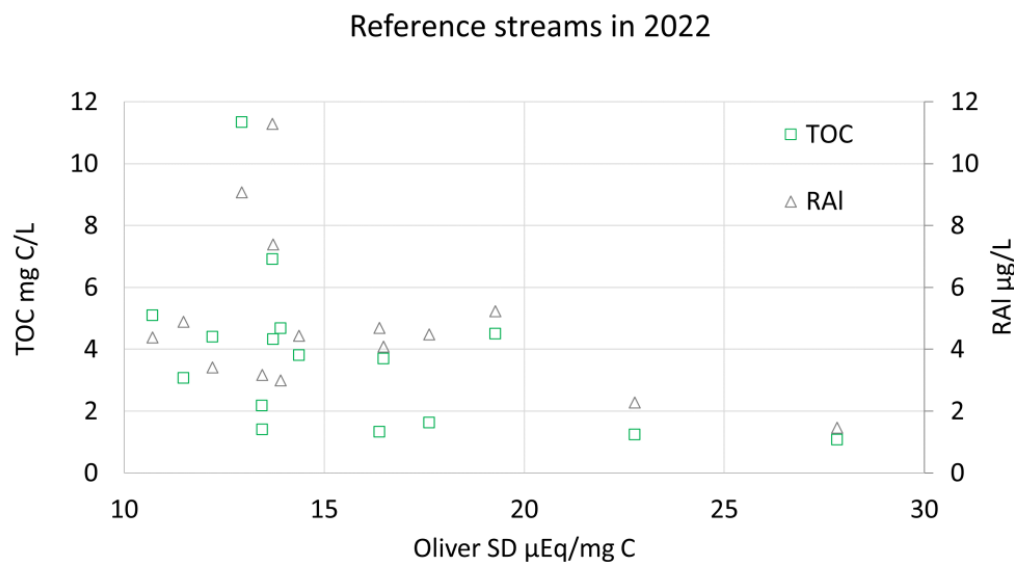


**Figure 5.** Relationship between concentrations of TOC and RAI vs. the optimized site density (SD) in the Oliver model at 16 Reference Streams in Norway. Based on monthly samples in 2022.

Among the 22 high-order rivers in the River Monitoring Program [26], coefficients of determination ( $R^2$ ) between  $OAN^-$  and  $Org^-$  exceeding 0.75 were only achieved in 10 sites. Rivers that failed to fit the model generally exhibited higher pH levels (median 7.36) and lower TOC concentrations (median 2.1 mg C/L) compared to rivers that demonstrated good explanatory values (median pH 6.84 and 3.2 mg C/L). The median SD values for the Oliver and Hruška models, fitted to monthly data from 2021 to 2023, were 11.0 and 12.6  $\mu\text{Eq}/\text{mg C}$ , respectively. These median contemporary values are lower than those observed in the upstream Reference Streams (13.8 and 15.8  $\mu\text{Eq}/\text{mg C}$  for the Oliver and Hruška models, respectively). Notably, as discussed below, the main difference lies in the CD, which exhibits considerably lower values in the high-order rivers compared to lower order streams, despite higher pH levels.

Samples with a specific color of DNOM (sVISA) less than 0.003 are typically associated with TOC concentrations of less than 5 mg C/L [30]. Consequently, the higher SD observed at sites with low TOC concentrations (Figure 5) can be conceptually explained by the relatively lower proportion of humic compared to fulvic fractions within the DNOM. The humic fraction, characterized by a lower SD, is more susceptible to changes in solubility compared to the hydrophilic fulvic fraction, as explained above. Consequently, the level of this fraction tends to be lower at sites exhibiting high ionic strength, low pH, and elevated RAI levels, commonly observed in acid-sensitive regions impacted by acid rain. This conceptual framework is supported by the observation that the optimized SD decreases with increasing sVISA, indicative of a greater relative proportion of humic compared to fulvic moieties in the DNOM within the Reference Streams dataset (Figure 6). On the other hand, a spatial Nordic study by Vogt et al. [31] noted that the specific UV absorbency (sUVA) tends to be lower in regions with heavy acid rain loading compared to less affected regions. This observation conflicts with our findings of lower median SD at sites impacted by acid rain (cf.  $H^+$  and RAI vs. SD in Figure 4 and Equations (10) and (12) and  $SO_4^{2-}$  relative to SD in Table 2), as a low sUVA implies DNOM with a relatively high fulvic acid fraction, which in turn entails a higher SD. This difference in spatial and temporal trends may partly be explained by regional differences in DNOM quality relative to temporal changes in organic Al complexation, as discussed below.

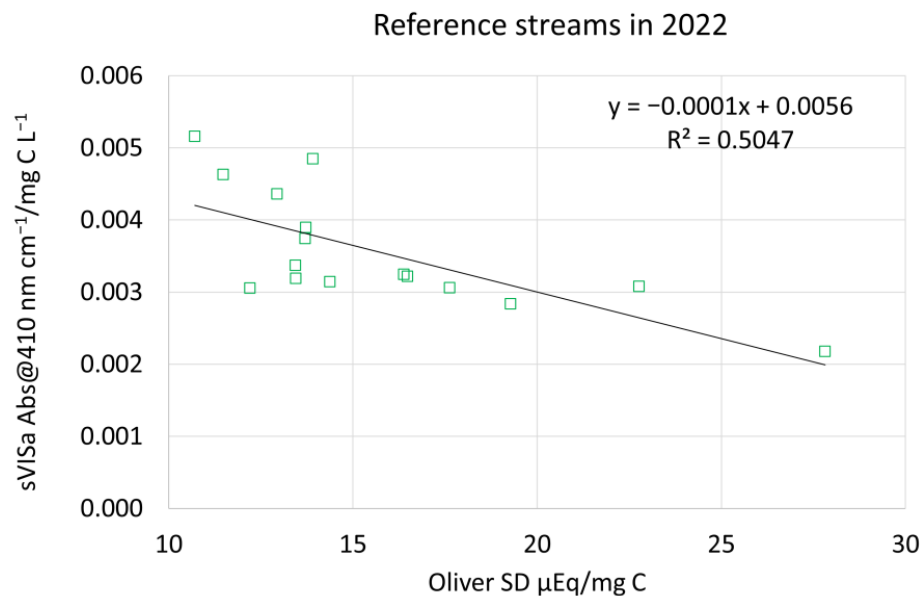


**Figure 6.** Correlation between specific visual absorbency (sVISA) and site density (SD) at 16 Reference Streams in Norway. The sVISA values are averaged monthly data from samples collected in 2022.

#### 4.6. Temporal Trends in Charge Density

Conceptually, the decline in acid rain loading has an antagonistic effect on the CD, as it leads to a decrease in SD due to an increase in humic moieties, while a concurrent increase in pH raises the relative protolysis ( $\alpha$ ) of the weak acid functional sites. Consequently, we would anticipate decreasing SD, while CD increases over time as acid rain diminishes. However, the decline in the organic complexation of Al, an unaccounted factor in the  $\text{OAN}^-$  models, serves as a confounding factor in assessing the impact of decreasing acid rain. The significance of this is highlighted by modelling the Al complexation to fulvic acids in the Birkenes stream water using the WHAM Model VII [32]. This model indicated a linear decline in organically complexed Al (NU) of  $7.2 \mu\text{mol Al}/\text{mg C}/\text{year}$ .

Simple linear temporal regression trends in the CD of the DNOM at the 78 Trend Lake sites reveal a median yearly increase (slope) of  $0.23 \mu\text{Eq}/\text{mg C}/\text{year}$ . Over the 34-year monitoring period, this translates to a cumulative rise of  $7.81 \mu\text{Eq}/\text{mg C}$ , signifying a doubling of the CD over time. In contrast, the  $\text{H}^+$  decreased by a median of  $5.26 \mu\text{Eq}/\text{L}$  from a median of  $5.62 \mu\text{Eq}/\text{L}$  in 1982 (equivalent to a change in pH from 5.25 in 1986 to 6.45 in 2020) in Norwegian Trend Lakes. Based on the Oliver model, this decrease of  $5.26 \mu\text{Eq H}^+/\text{L}$  results in a median CD increase of only  $0.761 \mu\text{Eq}/\text{mg C}$ . Hence, the observed increase in CD cannot be attributed to the enhanced deprotonation of weak acid functional groups. Since an increase in the humic to fulvic moieties of DNOM would mechanistically lead to a decrease in SD, the observed temporal rise in CD must, as also indicated above by the WHAM model, instead be attributed to reduced Al complexation with DNOM that was not accounted for in the model.

Spatial variations in the temporal CD slope, including samples with  $\text{Org.}^-$  set to 0, exhibit an exponential increase with decreasing ANC and TOC (Figure 7).

The pronounced temporal increases in the CD slope, exceeding  $2 \mu\text{Eq}/\text{mg C}/\text{year}$ , observed at Trend Lake sites characterized by low TOC concentrations (mainly  $< 1 \text{ mg C}/\text{L}$ ) and negative ANC (Figure 7), may, as discussed above for SD, partly stem from limitations inherent in the conceptual approach. Nonetheless, uncertainties in  $\text{Org.}^-$  calculations remain low in these acidic waters, given the negligible levels of bicarbonate. The notably higher increasing slope in CD observed in lakes with negative average ANC can largely be mechanistically explained by a temporal decrease in organic complexation with Al, as these waters with negative ANC tend to exhibit high LAI levels. Additionally, some deprotonation of weak acid functional groups with increasing pH could also contribute

to these high slopes. Still, the increases in CD at these acid-sensitive sites are thus likely more substantial than those observed at more well-buffered sites. It is noteworthy that this reduced organic Al complexation, which is not accounted for in the models, implies that also the apparent SD would likewise increase significantly over time.

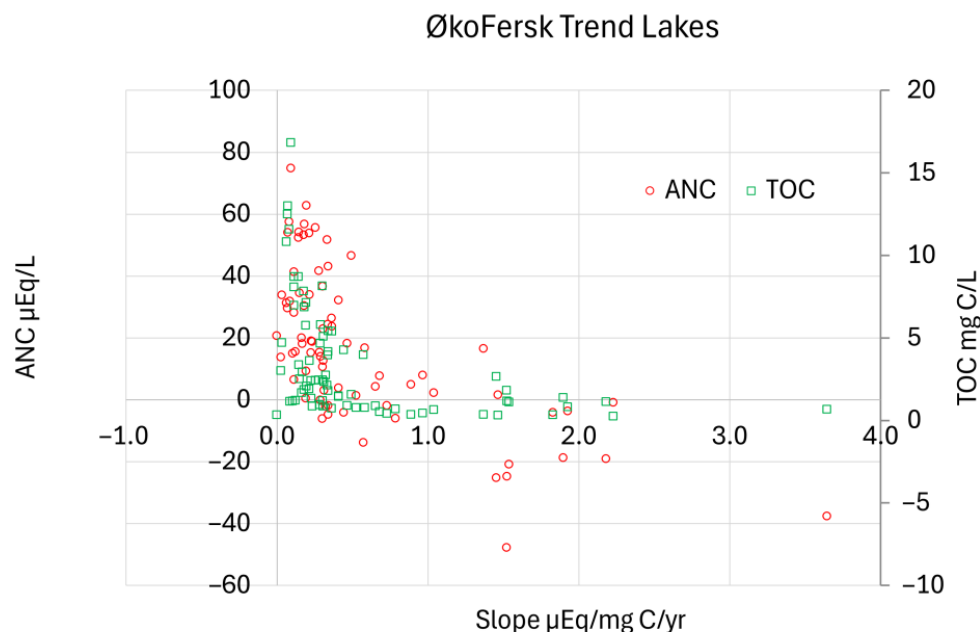


**Figure 7.** ANC and TOC as explanatory factors for spatial variation in the temporal slope of CD.

The intensively monitored Research Stations provide insights into both seasonal fluctuations and long-term trends at sites exhibiting variable acid sensitivity. A detailed summary of the simple temporal linear regression slopes in CD and key explanatory factors is presented in Table 3.

**Table 3.** Time trends in CD (i.e.,  $\text{Org.}^- / \text{TOC}$ ),  $\text{SO}_4^{2-}$ ,  $\text{H}^+$ , and the density of Al complexed to the DNOM (i.e.,  $\text{ILAI} / \text{TOC}$ ) at the 6 research monitoring stations between 2001 and 2021.

Station	CD Trend	$\text{SO}_4^{2-}$ Trend	$\text{H}^+$ Trend	ILAI/TOC Trend
	$\frac{\text{Eq}}{\text{mg C}} \frac{1}{\text{yr}}$	$\frac{\text{Eq}}{\text{L}} \frac{1}{\text{yr}}$	$\frac{\text{Eq}}{\text{L}} \frac{1}{\text{yr}}$	$\frac{\text{q ILAI}}{\text{mg C}} \frac{1}{\text{yr}}$
Birkenes	0.10	−1.93	−0.10	−0.47
Øygardsbekken	0.11	−1.13	−0.14	−0.31
Langtjern	0.01	−0.73	−0.02	−0.28
Storgama	0.06	−0.84	−0.19	−0.30
Kårvatn	−0.32	−0.16	0.00	−0.15
Dalelva	−0.17	−1.02	0.00	−0.20

Over the past two decades, changes in CD at the research monitoring sites have been significant relative to their average levels (Table 2). Particularly noteworthy is the increasing trend in CD at the most acid-rain-affected acid-sensitive sites, such as Birkenes, Øygardsbekken, and Storgama, which have experienced a substantial decline in  $\text{H}^+$  concentrations. These sites also demonstrate the largest decreases in Al complexation density on DNOM, indicated by declining ILAI/TOC ratios. There is a strong negative correlation between the trends in CD and  $\text{H}^+$ , explaining 58% of the variation, and between Al complexation density and CD, accounting for 71% of the variation among the six research monitoring stations. This increase in CD is therefore likely attributable to heightened deprotonation and reduced Al complexation resulting from the concurrent decrease in  $\text{H}^+$  concentrations and decline in ILAI/TOC, driven by the reduction in strong mineral acid loading (i.e., acid

rain). Although the models account for the effect of changes in pH, they do not incorporate the impact of decreased Al complexation. This diminished complexation's effect on the charged functional sites may contribute to some of the disparities between modelled  $\text{OAN}^-$  and calculated  $\text{Org.}^-$  values.

Conversely, there has been a general concurrent temporal increase in the color of DNOM, indicating a rise in the humic fraction relative to the fulvic acid fraction [33]. This trend likely constrains the increase in CD. Changes in climate may have had a similar effect by enhancing the influx of humic-rich allochthonous DNOM to surface waters. Terrestrial material typically exhibits a higher humic character than autochthonous material [31]. This shift is likely the cause for the strong decline in CD observed at the less acid-sensitive and acid-rain-loaded site of Kårvatn in central Norway. Dalelva, a non-acid-sensitive site, received heavy acid rain loading from the now-decommissioned metal smelter at Nikel in Russia. The temporal decline in CD at this site (Table 3) may be attributed to uncertainties in calculations due to low TOC concentrations and high pH, allowing for elevated bicarbonate concentrations. This aligns with the fact that the CDs at both sites are positively correlated to ANC, explaining 29% of the variation.

In summary, the CD of DNOM has significantly increased over the past 20 to 40 years, especially at acid-sensitive sites experiencing a reduction in acid deposition. Moreover, the primary governing parameters for the slope in CD differ between sites. In the acid-sensitive Trend Lakes, the main explanatory factors were ANC and TOC, whereas at the Research Monitoring Stations, which include both acid-sensitive and less acid-sensitive sites, the trends in CD were primarily explained by changes in acid rain loading, site acid sensitivity, and the density of Al complexed to DNOM.

These findings have implications for the expected future development of CD. The sUVa has been found to increase not only with decreasing acid deposition but also due to climate change [33]. This suggests that in areas where the influence of acid rain has been minimal, the SD and thus the CD have decreased with increasing DNOM, as observed in Kårvatn with low median sulphate levels (Table 2). Additionally, runoff from catchments with high biomass (forests) tends to have higher sUVa [16], resulting in lower SD. Furthermore, increased runoff and its intensity, especially through the forest floor containing DNOM with higher sUVa [31], could influence these trends. Consequently, it is reasonable to anticipate that SD and thus CD may decrease in the future due to the predicted climate changes.

## 5. Conclusions

The Oliver and Hruška organic charge models exhibit a strong explanatory value with calculated organic charge ( $\text{Org.}^-$ ) based on anion deficit. However, it is noteworthy that site density (SD) differs significantly across space and time (Table 4). This variation is due to disparities in the quality of DNOM, which arise from differences in the relative fractions of humic and fulvic moieties. Additionally, the charge neutralization of the anion base of these weak acid functional groups is influenced not only by pH but also by the density of aluminum (Al) complexed to the DNOM. While the impact of pH is relatively small and is predominantly accounted for by the models, the effect of decreased metal complexation is not addressed. The influence of Al complexation on the charge density (CD) of the DNOM may therefore explain some of the spatial differences in SD as well as the temporally increasing trends observed in acid-sensitive regions experiencing a decline in acid rain (Table 2).

This study highlights the complementary nature and practical utility of the conceptually grounded and empirically calibrated Oliver and Hruška models for estimating the charge concentration ( $\text{OAN}^-$ ) attributable to organic anions in dystrophic freshwaters. However, calibrating and testing these models has limitations at sites where the concentration of organic charge ( $\text{Org.}^-$ ) is low (i.e.,  $<20 \mu\text{Eq/L}$ ), such as in waters with low TOC ( $<1 \text{ mg C/L}$ ) or negative or low ANC and in hard waters enriched with base cations and bicarbonate. In cases where  $\text{Org.}^-$  significantly contributes to the ion balance (IB),

both the SD, used for model fitting, and the CD values exhibit temporal changes and spatial variations.

**Table 4.** Overview of optimized site (SD) and median charge density (CD) derived using the Oliver and Hruška models on the assessed Norwegian monitoring datasets.

Dataset	Site Type	Data Type	Period	# Sites	# Samples	Oliver SD	Hruška SD	Oliver CD	Hruška CD
Trend Lakes	Acid sensitive	Spatio-temporal	1986–2020	44	1 535	11.1	13.9	6.36	6.07
Reference Streams	Different land use	Spatio-temporal	2017–2023	35	1 310	14.4	16.3	12.0	12.2
Reference Streams	Different land use	Spatial	2022	16	181	13.8	15.8	12.3	13.6
Rivers	High order	Spatial	2021–2023	10	335	11.0	12.6	8.29	8.97

The provided differentiated estimates of SD and CD, reflecting identified governing factors, enable the more accurate modelling of DNOM charge. This is necessary for distinguishing its role in providing weak acid anions compared to bicarbonate in alkalinity assessments. Such evaluations are essential for understanding their contribution to biogeochemical processes such as enhanced weathering due to climate change. Additionally, as the charge density of organic matter increases, the efficiency of water treatment plants in removing DNOM from raw water decreases. Moreover, as levels of DNOM in many raw water sources continue to rise, drinking water treatment plants are forced to expand their treatment capacity and increase the coagulant dose. Better insight into factors governing CD aids these waterworks to tailor the dose required for the optimum removal of the DNOM. Likewise, a knowledge of the factors influencing changes in their DNOM quality enables drinking water treatment facilities to anticipate future quality shifts and adjust treatment processes accordingly. Moreover, water chemistry data users rely on charge balance to verify data quality. With organic charge typically accounting for 19% of the anion charge, such as in the 1000 Lakes survey, accurate assessments necessitate a reliable estimate of organic charge.

The improved estimates of site and charge density provided in this paper thus have significant practical implications for research on the environmental impacts of climate change, DNOM treatment in water treatment facilities, and the quality assurance of water chemistry data.

**Author Contributions:** Conceptualization, R.D.V. and Ø.A.G.; methodology, R.D.V. and Ø.A.G.; validation, R.D.V.; formal analysis, R.D.V. and Ø.A.G.; investigation, R.D.V., Ø.K., J.-E.T., K.A. and H.A.d.W.; data curation, L.B.S., J.E.S. and C.B.G.; writing—original draft preparation, R.D.V.; writing—review and editing, R.D.V., S.H., Ø.K., Ø.A.G., H.A.d.W., C.B.G. and K.A.; visualization, R.D.V.; project administration, R.D.V.; funding acquisition, R.D.V., H.A.d.W. and J.-E.T. All authors have read and agreed to the published version of the manuscript.

**Funding:** This research was funded by Royal Norwegian Ministry of Climate and Environment (project number 65007603I) for the ICP-Waters and the Norwegian Environment Agency (project number 21087345) including the following programs: ThousandLake survey, Monitoring long-range transboundary air pollution—Water chemical effects, the Norwegian River Monitoring Program, and the Surveillance monitoring of reference rivers. This research was also funded by a minor contribution by the Research Council of Norway (contract number 342628/L10).

**Data Availability Statement:** The data used in this analysis consist of historical records from 1986 to 2020 that may be sourced from [https://github.com/JamesSample/icpw2/tree/master/thematic\\_report\\_2023](https://github.com/JamesSample/icpw2/tree/master/thematic_report_2023) and <https://vannmiljo.miljodirektoratet.no/>. The 1000 Lakes data are available at zenodo.org with the following DOI: <https://doi.org/10.5281/zenodo.7298477>.

**Acknowledgments:** Numerous individuals, too many to list here, have dedicated considerable time and effort over two decades to carry out water sampling, meticulously manage laboratory procedures and analyses, and oversee database management. Their collective contributions have been instrumental in generating the high-quality monitoring data upon which this work depends.

**Conflicts of Interest:** The authors declare no conflicts of interest. The funders had no role in the design of the study; in the collection, analyses, or interpretation of data; in the writing of the manuscript; or in the decision to publish the results.

## References

1. Monteith, D.T.; Henrys, P.A.; Hruška, J.; de Wit, H.A.; Krám, P.; Moldan, F.; Posch, M.; Räike, A.; Stoddard, J.L.; Shilland, E.M.; et al. Long-term rise in riverine dissolved organic carbon concentration is predicted by electrolyte solubility theory. *Sci. Adv.* **2023**, *9*, eade3491. [[CrossRef](#)] [[PubMed](#)]
2. Madsen, H.; Lawrence, D.; Lang, M.; Martinkova, M.; Kjeldsen, T.R. Review of trend analysis and climate change projections of extreme precipitation and floods in Europe. *J. Hydrol.* **2014**, *519*, 3634–3650. [[CrossRef](#)]
3. De Wit, H.A.; Garmo, Ø.A.; Jackson-Blake, L.; Clayer, F.; Vogt, R.D.; Kaste, Ø.; Gundersen, C.B.; Guerrero, J.L.; Hindar, A. Changing Water Chemistry in One Thousand Norwegian Lakes During Three Decades of Cleaner Air and Climate Change. *Glob. Biogeochem. Cycles* **2023**, *37*, e2022GB007509. [[CrossRef](#)]
4. Kritzberg, E.S.; Hasselquist, E.M.; Škerlep, M.; Löfgren, S.; Olsson, O.; Stadmark, J.; Valinia, S.; Hansson, L.-A.; Laudon, H. Browning of freshwaters: Consequences to ecosystem services, underlying drivers, and potential mitigation measures. *Ambio* **2020**, *49*, 375–390. [[CrossRef](#)] [[PubMed](#)]
5. Klante, C. Hydrophysical Processes Governing Brownification—A Case Stud of Lake Bolmen, Sweden. Ph. D. Thesis, Lund University, Lund, Sweden, 2023.
6. Eklöf, K.; von Brömssen, C.; Amvrosiadi, N.; Fölster, J.; Wallin, M.B.; Bishop, K. Brownification on hold: What traditional analyses miss in extended surface water records. *Water Res.* **2021**, *203*, 117544. [[CrossRef](#)] [[PubMed](#)]
7. Reuss, J.O.; Johnson, D.W. Acid Deposition and the Acidification of Soils and Waters. In *Ecological Studies*; Springer: Berlin, Germany, 1986; Volume 59, p. 119.
8. Lydersen, E.; Larssen, T.; Fjeld, E. The influence of total organic carbon (TOC) on the relationship between acid neutralizing capacity (ANC) and fish status in Norwegian lakes. *Sci. Total Environ.* **2004**, *326*, 63–69. [[CrossRef](#)] [[PubMed](#)]
9. Kastl, G.; Sathasivan, A.; Fisher, I.; Van Leeuwen, J. Modeling DOC Removal Enhanced Coagulation. *J.-Am. Water Work. Assoc.* **2004**, *96*, 79–89. [[CrossRef](#)]
10. Brakke, D.; Henriksen; Norton, S. The relative importance of acidity sources for humic lakes in Norway. *Nature* **1987**, *329*, 432–434. [[CrossRef](#)]
11. Henriksen, A.; Seip, H.M. Strong and weak acids in surface waters of southern Norway and southwestern Scotland. *Water Res.* **1980**, *14*, 809–813. [[CrossRef](#)]
12. Kortelainen, P. Charge-density of total organic carbon in Finnish lakes. *Environ. Pollut.* **1992**, *77*, 107–113. [[CrossRef](#)]
13. Hruška, J.; Köhler, S.; Laudon, H.; Bishop, K. Is a Universal Model of Organic Acidity Possible: Comparison of the Acid/Base Properties of Dissolved Organic Carbon in the Boreal and Temperate Zones. *Environ. Sci. Technol.* **2003**, *37*, 1726–1730. [[CrossRef](#)]
14. Oliver, B.G.; Thurman, E.M.; Malcolm, R.L. The contribution of humic substances to the acidity of colored natural waters. *Geochim. Et Cosmochim. Acta* **1983**, *47*, 2031–2035. [[CrossRef](#)]
15. Perdue, E.M.; Ritchie, J.D. *Treatise on Geochemistry*; Heinrich, D.H., Karl, K.T., Eds.; Pergamon: Oxford, UK, 2003; Chapter 5.10; pp. 273–318.
16. Vogt, R.D.; Porcal, P.; Hejzlar, J.; Paule-Mercado, M.C.; Haaland, S.; Gundersen, C.B.; Orderud, G.I.; Eikebrokk, B. Distinguishing between Sources of Natural Dissolved Organic Matter (DOM) Based on Its Characteristics. *Water* **2023**, *15*, 3006. [[CrossRef](#)]
17. Hindar, A.; Larssen, T. Modification of ANC- and critical load assessments by including strong organic acids. NIVA-report. *Naturens Tålegrenser*. **2005**, 5030. (In Norwegian)
18. Driscoll, C.T.; Lehtinen, M.D.; Sullivan, T.J. Modelling the acid-base chemistry of organic solutes in Adirondack, New York, lakes. *Water Resour. Res.* **1994**, *30*, 297–306. [[CrossRef](#)]
19. Schecher, W.D.; Driscoll, C.T. An evaluation of uncertainty associated with aluminum equilibrium calculations. *Water Resour. Res.* **1987**, *23*, 525–534. [[CrossRef](#)]
20. Kortelainen, P. Content of Total Organic Carbon in Finnish Lakes and Its Relationship to Catchment Characteristics. *Can. J. Fish. Aquat. Sci.* **1993**, *50*, 1477–1483. [[CrossRef](#)]
21. Tipping, E. WHAMC—A chemical equilibrium model and computer code for waters, sediments, and soils incorporating a discrete site/electrostatic model of ion-binding by humic substances. *Comput. Geosci.* **1994**, *20*, 973–1023. [[CrossRef](#)]
22. Tipping, E. *Cation Binding by Humic Substances*; Cambridge University Press: Cambridge, UK, 2002.
23. Kinniburgh, D.G.; van Riemsdijk, W.H.; Koopal, L.K.; Borkovec, M.; Benedetti, M.F.; Avena, M.J. Ion binding to natural organic matter: Competition, heterogeneity, stoichiometry, and thermodynamic consistency. *Colloids Surf. A* **1999**, *151*, 147–166. [[CrossRef](#)]
24. Vogt, R.D.; Agnieszka, K.; Arle, J.; Austnes, K.; Van Dam, H.; Futter, M.; Fölster, J.; Gundersen, C.B.; Higgins, S.N.; Houle, D.; et al. *Trends and Patterns in Surface Water Chemistry in Europe and North America between 1990 and 2020, with a Focus on Calcium*; Report No. ICP Waters Report 156/2024, 65; Norwegian Institute for Water Research: Oslo, Norway, 2024.
25. Sandin, L.; Thrane, J.-E.; Persson, J.; Kile, M.R.; Bækkelie, K.A.; Myrvold, K.M.; Garmo, Ø.A.; Grung, M.; Calidonio, J.-L.; de Wit, H.; et al. *Monitoring of Reference Rivers—Testing of the Classification System for Basic Monitoring in Reference Watercourses*; 243/2021; Norwegian Institute for Water Research: Oslo, Norway, 2021. (In Norwegian)



26. Kaste, Ø.; Gundersen, C.B.; Sample, J.E.; McGovern, M.; Skancke, L.B.; Allan, I.; Jenssen, M.T.S.; Bæk, K.; Skogan, O.A.S. *The Norwegian River Monitoring Programme 2022—Water Quality Status and Trends. Elveovervåkningsprogrammet 2022—Vannkvalitetstilstand Og-Trender*; NIVA-rapport 7903-2023; Norwegian Institute for Water Research: Oslo, Norway, 2023.
27. Norwegian Environment Agency. Vannmiljø Database. Available online: <https://vannmiljo.miljodirektoratet.no/> (accessed on 5 June 2024).
28. Vogt, R.D.; Garmo, Ø.A.; Schartau, A.K.; Haaland, S.L. Methods for calculating the water acid neutralizing capacity (ANC) for classification of acidification status. *Vann* **2023**, *02/58*, 105–117. (In Norwegian)
29. *EN ISO 9963-1:1994; Water Quality—Determination of Alkalinity—Part 1: Determination of Total and Composite Alkalinity*. ISO: Geneva, Switzerland.
30. Kaste, Ø.; Skarbøvik, E.; Vogt, R.D. *Investigation on Parameters for Suspended Matter and Organic Material That Can Be Included in the Water Classification System*; Report 58 (NIVA Report 7860-2023); Norwegian Institute for Water Research: Oslo, Norway, 2023. (In Norwegian)
31. Vogt, R.D.; Akkanen, J.; Andersen, D.O.; Bruggemann, R.; Chatterjee, B.; Gjessing, E.; Kukkonen, J.V.K.; Larsen, H.E.; Luster, J.; Paul, A.; et al. Key site variables governing the functional characteristics of dissolved natural organic matter (DNOM) in Nordic forested catchments. *Aquat. Sci.* **2004**, *66*, 195–210. [[CrossRef](#)]
32. Tipping, E.; Lofts, S.; Sonke, E. Humic Ion-Binding Model VII: A revised parameterisation of cation-binding by humic substances. *Environ. Chem.* **2011**, *8*, 225–235. [[CrossRef](#)]
33. Hongve, D.; Riise, G.; Kristiansen, J. Increased colour and organic acid concentrations in Norwegian forest lakes and drinking water—A result of increased precipitation? *Aquat. Sci.* **2004**, *66*, 231–238. [[CrossRef](#)]

**Disclaimer/Publisher’s Note:** The statements, opinions and data contained in all publications are solely those of the individual author(s) and contributor(s) and not of MDPI and/or the editor(s). MDPI and/or the editor(s) disclaim responsibility for any injury to people or property resulting from any ideas, methods, instructions or products referred to in the content.